applied sciences

MDPI

Article

Spotted Hyena Optimizer and Ant Lion Optimization in Predicting the Shear Strength of Soil

Hossein Moayedi [1,2,*], Dieu Tien Bui [3,4,*], Dounis Anastasios [5] and Bahareh Kalantar [6]

1 Department for Management of Science and Technology Development, Ton Duc Thang University, Ho Chi Minh 758307, Vietnam
2 Faculty of Civil Engineering, Ton Duc Thang University, Ho Chi Minh 758307, Vietnam
3 Institute of Research and Development, Duy Tan University, Da Nang 550000, Vietnam
4 Geographic Information System Group, Department of Business and IT, University of South-Eastern Norway, N-3800 Bø i Telemark, Norway
5 Deptartment of Industrial Design and Production Engineering, University of West Attica, Campus 2250 Thivon & P. Ralli, 12244 Egaleo, Greece; aidounis@uniwa.gr
6 RIKEN Center for Advanced Intelligence Project, Goal-Oriented Technology Research Group, Disaster Resilience Science Team, Tokyo 103-0027, Japan; bahareh.kalantar@riken.jp
* Correspondence: hossein.moayedi@tdtu.edu.vn (H.M.); buitiendieu@duytan.edu.vn (D.T.B.); Tel.: +47-96-677678 (D.T.B.)

Received: 15 September 2019; Accepted: 2 November 2019; Published: 6 November 2019

Abstract: Two novel hybrid predictors are suggested as the combination of artificial neural network (ANN), coupled with spotted hyena optimizer (SHO) and ant lion optimization (ALO) metaheuristic techniques, to simulate soil shear strength (SSS). These algorithms were applied to the ANN for counteracting the computational drawbacks of this model. As a function of ten key factors of the soil (including depth of the sample, percentage of sand, percentage of loam, percentage of clay, percentage of moisture content, wet density, liquid limit, plastic limit, plastic Index, and liquidity index), the SSS was considered as the response variable. Followed by development of the ALO–ANN and SHO–ANN ensembles, the best-fitted structures were determined by a trial and error process. The results demonstrated the efficiency of both applied algorithms, as the prediction error of the ANN was reduced by around 35% and 18% by the ALO and SHO, respectively. A comparison between the results revealed that the ALO–ANN (Error = 0.0619 and Correlation = 0.9348) performs more efficiently than the SHO–ANN (Error = 0.0874 and Correlation = 0.8866). Finally, an SSS predictive formula is presented for use as an alternative to the difficult traditional methods.

Keywords: swarm intelligence; metaheuristic optimization; nature-inspired; soil shear strength; artificial intelligence

1. Introduction

Utilizing artificial intelligence as an inexpensive yet accurate model has attracted the attention of scientists. The efficiency of machine learning approaches has been proved for modeling various geotechnical parameters including the soil shear strength (SSS) [1]. Moayedi and Hayati [2] successfully used various machine learning techniques for predicting the ultimate bearing capacity of strip footing near a slope. The same authors investigated the feasibility of some artificial intelligence tools like the support vector machine (SVM) and the adaptive neuro-fuzzy inference system (ANFIS) for modeling the friction capacity of a driven pile in clay [3]. The SSS is one of the most significant parameters, and needs to be meticulously evaluated for stability analysis of soil in geotechnical and more comprehensive civil engineering projects e.g., retaining walls and road foundations and pavements [4,5]. More specifically, it indicates the internal resistance of soil against failure and sliding along any internal plane [6]. The high

significance of measuring this parameter for designing different parts of a structure, like foundation [7], has driven engineers to pay special attention to the SSS. On the other hand, determining the SSS-related parameters by laboratory tests is a complicated task and mainly requires performing destructive tests. Moreover, high spending costs [8], as well as learning special skills for working with complex apparatus [9–12] are other disadvantages of direct approaches for SSS measurement.

Conventional models (like multivariate approaches [13] and empirical methods [14]) have been widely used as SSS evaluative models. Also, in studies carried out by Zhai et al. [15] and Al Aqtash and Bandini [16], a model for forecasting unsaturated shear strength was suggested based on the soil-water characteristic curve. Likewise, some evaluative models based on the soil-water retention curve (SWRC) have been explored by Garven and Vanapalli [17]. In the case of intelligent models, plenty of research has been conducted to estimate this parameter. Kiran et al. [18] demonstrated the efficacy of probabilistic neural networks for the SSS simulation. In that study, they deemed plasticity index, water content, dry density, and the percentage of some factors such as sand, gravel, clay, and silt as input factors. In a study by Jokar and Mirasi [19], the applicability of two clustering methods of ANFIS, including fuzzy c-mean clustering and subtractive clustering, was examined for estimating the shear strength of unsaturated soils. Kanungo et al. [20] compared the sufficiency of the ANN and the regression tree (CART) for simulating unsaturated SSS and found that the ANN is the superior model. Besalatpour et al. [21] compared the potential of the ANN and the ANFIS for predicting the SSS from measured particle size distribution, normalized difference vegetation index (NDVI), soil organic matter (SOM), and calcium carbonate equivalent (CCE). The superiority of the ANN was revealed, referring to the calculated error, as well as the correlation values (0.05 and 0.86 for the ANN, and 0.08 and 0.60 for the ANFIS).

Utilizing different linear and nature-inspired algorithms (like blind naked mole-rat (BNMR) and SIRT algorithms) enabled the scientists to better deal with various engineering issues [22,23]. Furthermore, many scholars have proven that the incorporation of hybrid metaheuristic algorithms with a regular predictive algorithm can result in computational drawbacks like local minima [24–27]. Studies such as [28,29] have demonstrated the potential of the ANFIS to be hybridized in order to naturalize hazard modeling, such as landslide and flood hazards. In the field of SSS, different works have explored the use of hybrid models for optimizing typical predictors. In this sense, Bui et al. [30] investigated the feasibility of the incorporation of SVM-based models with metaheuristic algorithms, and showed that the cuckoo search optimization (CSO) enhances the accuracy of the least squares support vector machine (LSSVM). It was also revealed that the ensemble of CSO-LSSVM (R^2 = 0.885 and RMSE = 0.082) performs more efficiently than the ANN and the regression tree (RT) for predicting the SSS. Likewise, Nhu et al. [7] explored the combination of particle swarm optimization (PSO) along with the support vector regression (SVR) and found that the suggested ensemble is a robust model for the design aims. This model also surpassed the benchmark models of ANN, RT, ANFIS, and multivariate adaptive regression splines. The applicability of PSO and a genetic algorithm for optimizing the ANFIS, and for approximating the clay SSS of two bridge construction projects (in Vietnam) was examined by Pham et al. [31]. Their findings showed that both hybridized ANFIS networks perform more successfully than the SVR and ANN.

The present study fills the gap of knowledge related to employing novel hybrid techniques for optimizing the performance of an artificial neural network toward indirect measurement of the SSS. Despite the wide application of popular optimization algorithms like the PSO and GA, the authors did not come across any previous research focusing on the robustness evaluation of recently developed algorithms like the spotted hyena optimizer (SHO) and ant lion optimization (ALO) in the aforementioned fields. Hence, these algorithms are applied to an ANN to optimize its computational weights and biases when it is utilized to predict the SSS using real-world soil information.

2. Methodology

As was explained previously, in this work, two metaheuristic algorithms were coupled with artificial neural networks to create the neural ensembles of ALO–ANN and SHO–ANN. MATLAB 2014 was used to develop the algorithms. Figure 1 illustrates the steps taken to fulfill the purpose of this research. The networks were then fed by these data to find the relationship between the dependent and independent variables. Next, the best complexity of the predictive models was determined by a trial and error process. Lastly, the results were evaluated and analyzed using three well-known accuracy criteria, namely, root mean square error (RMSE), mean absolute error (MAE), and the coefficient of determination (R^2). Assuming N as the number of samples, $Y_{i_{predicted}}$ and $Y_{i_{observed}}$ as the predicted and observed SSSs, and $\overline{Y}_{observed}$ as the mean value of the $Y_{i_{observed}}$, Equations (1)–(3) describe these indices. Moreover, the ruling equation of the best-fitted model is presented for use as the SSS predictive formula.

$$RMSE = \sqrt{\frac{1}{N}\sum_{i=1}^{N}\left[\left(Y_{i_{observed}} - Y_{i_{predicted}}\right)\right]^2} \quad (1)$$

$$MAE = \frac{1}{N}\sum_{I=1}^{N}\left|Y_{i_{observed}} - Y_{i_{predicted}}\right| \quad (2)$$

$$R^2 = 1 - \frac{\sum_{i=1}^{N}\left(Y_{i_{predicted}} - Y_{i_{observed}}\right)^2}{\sum_{i=1}^{N}\left(Y_{i_{observed}} - \overline{Y}_{observed}\right)^2} \quad (3)$$

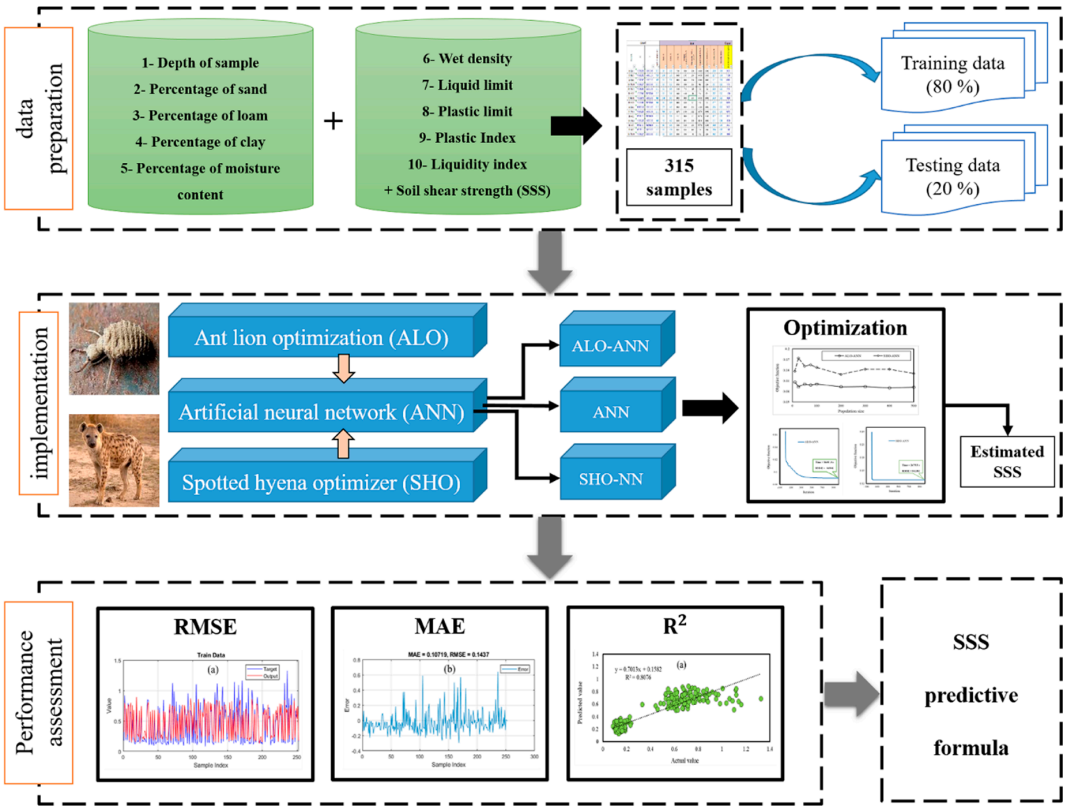

Figure 1. The steps taken for soil shear strength (SSS) simulation in this study.

The methodology of the used models is described below:

2.1. Artificial Neural Network

An artificial neural network (ANN) mimics the human neural system [32] to make an intelligent processor capable of being used for many regression and classification aims with complicated non-linear conditions [33]. The high prediction capability of the ANN has made its different notions popular for various engineering simulations [34–38]. Multi-layer perceptron (MLP) is known as the most common type of ANN. As the name denotes, this network comprises some layers with a number of computational units called "neurons." The back-propagation learning method [39], as well as the Levenberg–Marquardt training algorithm [40–42], enable the ANN to discern the relationship between the input and output parameters. In this sense, we allowed T_k and O_k to be the target and modelled a response in the neuron k, χ_k is obtained by Equation (4):

$$\chi_k = O_k(1 - O_k)(O_k - T_k) \tag{4}$$

Next, assuming W_{mk} as the weight connecting the nodes m and k, λ_m is calculated as follows in the sandwiched layer:

$$\lambda_m = O_m(1 - O_m)\sum_k \chi_k W_{mk} \tag{5}$$

The weights and biases are then adjusted using Equations (6) and (7):

$$W' = W + \Delta W \tag{6}$$

$$b' = b + \Delta b \tag{7}$$

Let L and q represent the layer and learning rate, respectively, ΔW and Δb are then computed as follows:

$$\Delta W = -q\ \chi_L\ L_{L-1} \tag{8}$$

$$\Delta b = -q\ \chi_L \tag{9}$$

2.2. Metaheuristic Algorithms

2.2.1. Spotted Hyena Optimizer

Proposed by Dhiman and Kumar [43], the spotted hyena optimizer (SHO) is a recently developed optimization technique that is inspired by the hunting behavior of the spotted hyena. Spotted hyena are social animals that usually live and hunt in groups. The main stages of this algorithm include searching for prey, encircling prey, attacking prey, and other searching behaviors of spotted hyenas (Figure 2). During this process, the most promising candidate solution is considered to be the aimed for prey or the objective near the optimum because the search space is not known a priori [43]. In the SHO, it is assumed that the elite search agent knows about the prey location and other individuals try to update their positions by making a cluster—reliable group of friends—towards the elite agent. Further information about the ruling equations of the SHO can be found in previous studies [44–46].

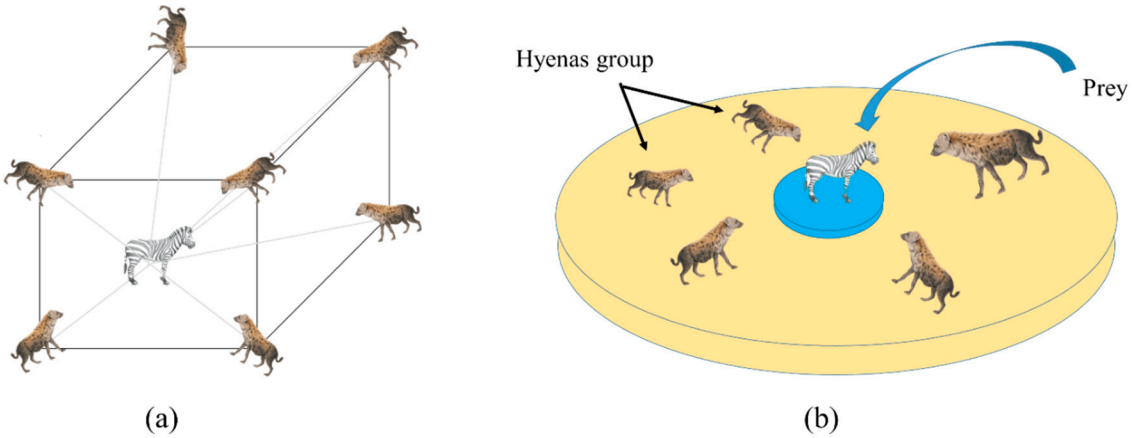

Figure 2. Hunting process carried out in the spotted hyena optimizer (SHO) algorithm: (**a**) position vectors and the possible next locations of the members, and (**b**) attacking the prey.

2.2.2. Ant Lion Optimization

Imitating the herding behavior of ant lions in their larvae life period, Mirjalili [47] developed the ant lion optimization (ALO) algorithm as a new capable metaheuristic technique. In the ALO, primary locations of the target hunt and ant lions are stochastically defined in the existing search space. This algorithm comprises six steps in each repetition including: (a) a random walk of prey, (b) trapping in holes, (c) constructing a trap, (d) the sliding of prey towards the ant lion, (e) catching the prey/reconstructing the hole, and (f) determining the elite ant lion. Figure 3 illustrates the first stage, along with the hunting behavior of antlions. The fitness of the prey is contributed to the hunting capability of the ant lions. This is because it is supposed that each hunter hunts one prey. A so-called function "roulette wheel selection (RWS)" is applied for this purpose. Further details of the ALO and the mathematical optimization process are detailed in other studies, such as [48–50].

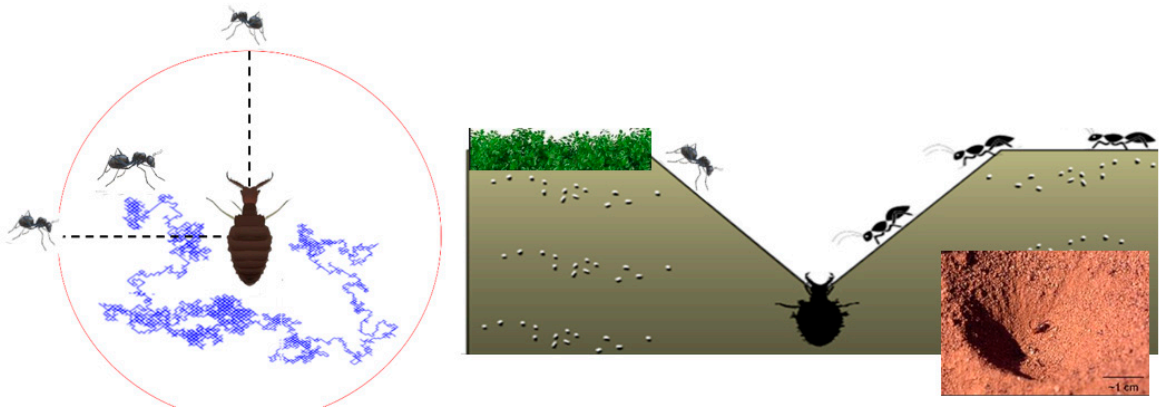

Figure 3. (**a**) Random walk of the prey inside the trap, and (**b**) the hunting behavior of antlions.

3. Data Collection and Statistical Analysis

The dataset used to train the intelligent models of the current research was provided by a geotechnical survey in a road construction project, based on a study by Bui et al. [30]. More clearly, the Trung Luong National Expressway section was selected as the case study, which forms 81 to 87 km of the Ho Chi Minh–Can Tho Expressway in the Mekong River delta, Vietnam. A total of 73 boreholes were drilled, where the maximum and minimum depths were 70.5 and 12.5, respectively. The tests

carried out for obtaining the information were the vane shear test [51], the cone penetration test [52], and the standard penetration test [53].

Considering the 10 key factors of soil, namely depth of sample (DOP), percentage of sand, percentage of loam, percentage of clay, percentage of moisture content (MC), wet density (WD), liquid limit (LL), plastic limit (PL), plastic Index (PI), and liquidity index (LI) as input variables, the shear strength is estimated as the target variable. After data pre-processing, the dataset consisted of 315 samples. Out of those, 80% (i.e., 252 samples) were randomly selected for pattern recognition by the intelligent models (i.e., the training process), and the remaining 20% (i.e., 63 samples) were set aside to evaluate the capability of the implemented models for pattern prediction (i.e., the testing process). Figure 4 illustrates the histogram charts of the input and output variables. Table 1 denotes the descriptive statistics of the used dataset.

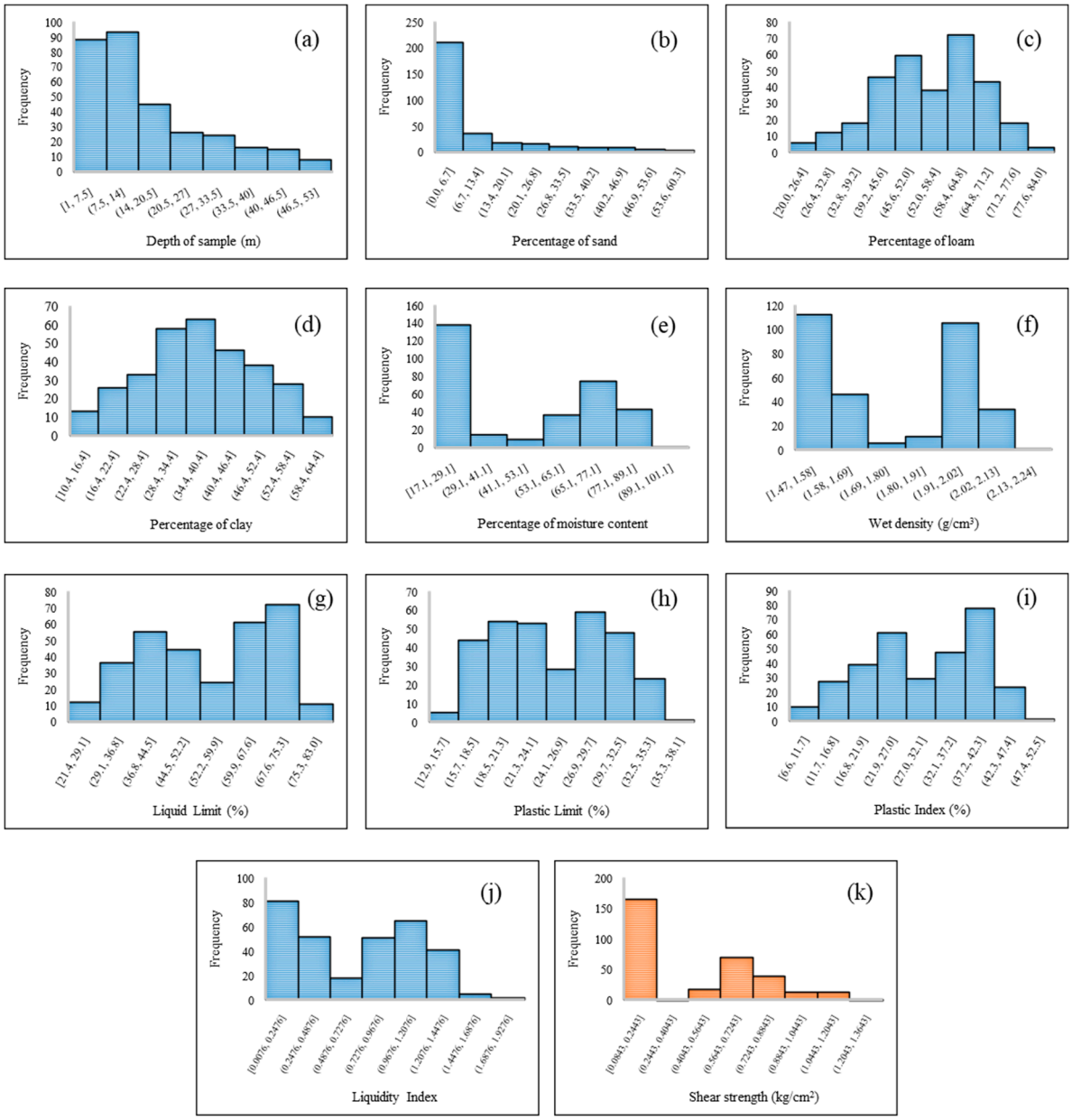

Figure 4. Histogram of (**a**) depth of sample, (**b**) percentage of sand, (**c**) percentage of loam, (**d**) percentage of clay, (**e**) percentage of moisture content, (**f**) wet density, (**g**) liquid limit, (**h**) plastic limit, (**i**) plastic Index, (**j**) liquidity index, and (**k**) shear strength.

Table 1. Descriptive statistics of the used dataset.

Features	Descriptive Index							
	Mean	Standard Error	Median	Standard Deviation	Sample Variance	Skewness	Minimum	Maximum
Depth of sample (m)	16.21	0.71	13.00	12.57	157.94	1.02	1.00	52.00
Sand (%)	8.40	0.73	2.40	13.04	169.92	1.85	0.00	57.30
Loam (%)	54.01	0.70	56.10	12.46	155.30	−0.30	20.00	83.70
Clay (%)	37.28	0.66	37.60	11.68	136.35	0.01	10.40	63.90
Moisture content (%)	48.47	1.35	49.90	23.90	571.41	0.12	17.10	90.30
Wet density (g/cm^3)	1.77	0.01	1.69	0.21	0.05	0.09	1.47	2.15
Liquid limit (%)	54.47	0.84	54.90	14.89	221.65	−0.23	21.40	79.90
Plastic limit (%)	24.72	0.30	24.40	5.39	29.05	0.02	12.90	35.90
Plastic Index (%)	29.75	0.56	30.40	10.00	99.92	−0.27	6.60	49.70
Liquidity index	0.70	0.03	0.79	0.46	0.22	0.04	0.01	1.73
Shear strength (kg/cm^2)	0.43	0.02	0.21	0.32	0.10	0.55	0.08	1.33

4. Results and Discussion

4.1. Optimizing the MLP using ALO and SHO

As mentioned supra, this study addressed two novel optimizations of artificial neural networks for counteracting its computational drawbacks in the modeling of the soil shear strength. To optimize the ANN, the ALO and SHO metaheuristic techniques are incorporated with it. However, determining the best structure of the ANN is a prerequisite for this task. Based on the authors' experience, as well as a trial and error process, an MLP neural network with five computational units in the hidden layer was selected as the most suitable structure.

Next, the ANN was given to the proposed optimization techniques to develop the ALO–ANN and SHO–ANN hybrid ensembles. Note that the computational parameters (i.e., the connecting weights and biases) were the variables of the problem. In other words, the ALO and SHO were performed to find the best values for them. In this way, the number of repetitions was set at 1000, and the RMSE between the actual and predicted SSSs was defined as the objective function. Of note, a population-based trial and error process was also carried out to determine the best-fitted complexity of each ensemble. The models were tested by nine population sizes varying from 10 to 500 (10, 25, 50, 75, 100, 200, 300, 400, and 500), and the RMSE of the latest iteration was recorded. The results are shown in Figure 5a. According to this figure, there is a considerable distinction between the results of the ALO and SHO. As shown, the lowest RMSEs of the models were obtained for the ALO–ANN with population size = 400, and the SHO–ANN with population size = 200 (RMSEs were 0.090138704 and 0.128263102, respectively.) This indicates that the solution suggested by these complexities constructs a more promising ANNS. For more details, Figure 5b,c depicts the convergence curves of the elite structure of the mentioned algorithms.

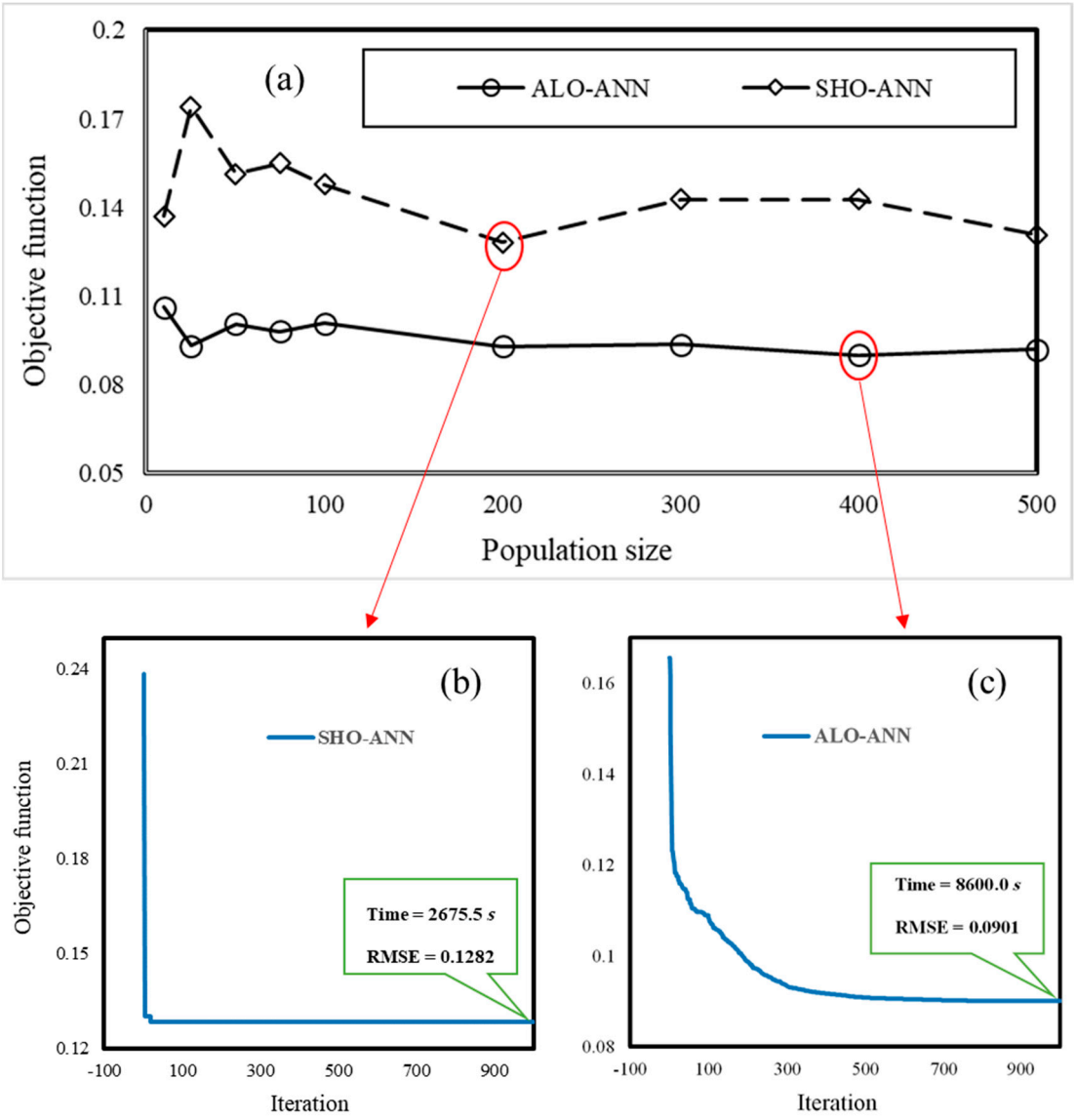

Figure 5. (**a**) The results of the executed trial and error process, (**b**,**c**) the convergence curve of the elite SHO–ANN and ALO–ANN, respectively. ANN, artificial neural network; ALO, ant lion optimization.

4.2. Quality Assessment of Predictive Models

The best-fitted structure of the ANN, ALO–ANN, and SHO–ANN was then used to predict the SSS using the considered input factors. The comparison between the actual and predicted SSSs was made in this section to evaluate the efficiency of the implemented models. Firstly, the RMSE and MAE error criteria were used to measure the error of the performance, and the R^2 was then applied to measure the correlation between the target and output variables.

The results of the ANN, ALO–ANN, and SHO–ANN are shown in Figures 6–8, respectively. Evaluating the obtained values' error criteria in the training phase shows that applying the metaheuristic algorithms has effectively helped the ANN to achieve a more reliable analysis of the relationship between the SSS and influential factors. In detail, the RMSE of the ANN decreased by around 37% and 11% (i.e., from 0.1437 to 0.0901 and 0.1282) as a result of the ALO and SHO, respectively. The results of the MAE also agree with the RMSE and experienced a reduction by nearly 47% and 17% (i.e., from 0.1071 to 0.0563 and 0.0892). Comparing the error charts (showing the difference between the actual and predicted values for each sample) also indicates that the ensemble models have trained the ANN better than its regular algorithms.

The testing results demonstrate that the errors of the ALO–ANN and SHO–ANN are lower than ANN. More clearly, the RMSE levelled off from 0.1603 to 0.1035 (35.43%) and 0.1308 (18.40%). As for the MAE, the ALO and SHO reduced it from 0.1268 to 0.0619 (51.18%) and 0.0874 (31.07%). It points out that the networks constructed by the developed ensembles are more capable than unreinforced ANN in predicting unseen soil conditions. Graphically, part (c) of Figures 6–8 shows that the products of the ensemble models have better agreement with the actual SSSs.

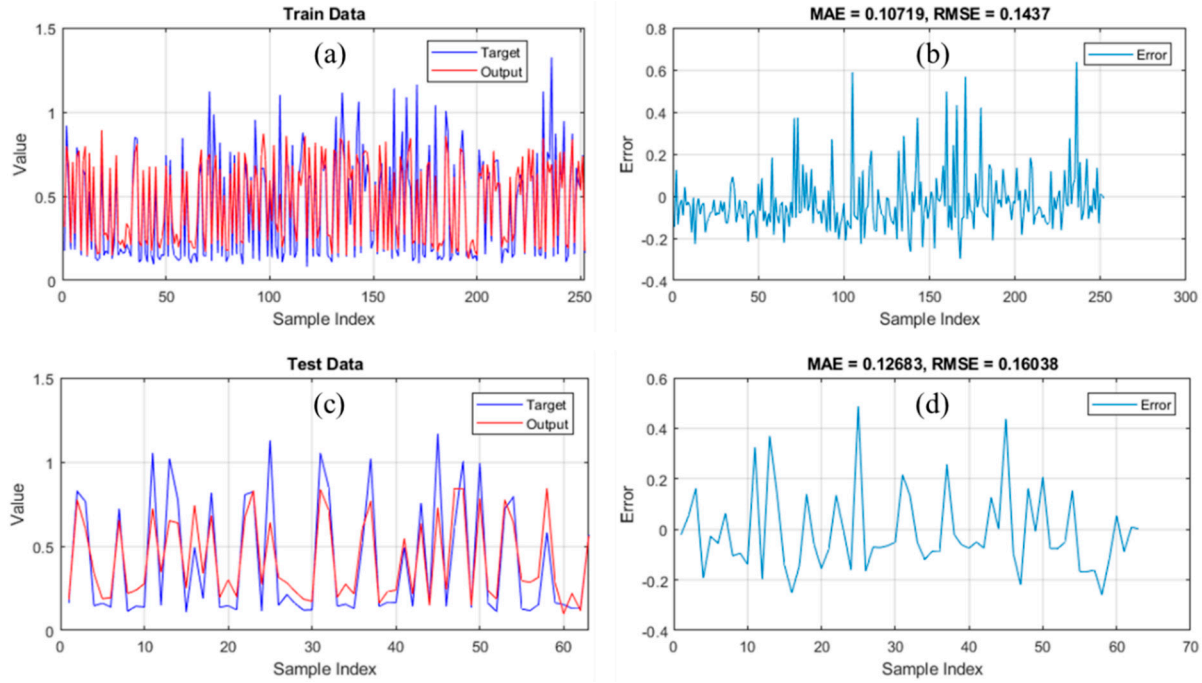

Figure 6. The ANN results for the (**a**,**b**) training and (**c**,**d**) testing data.

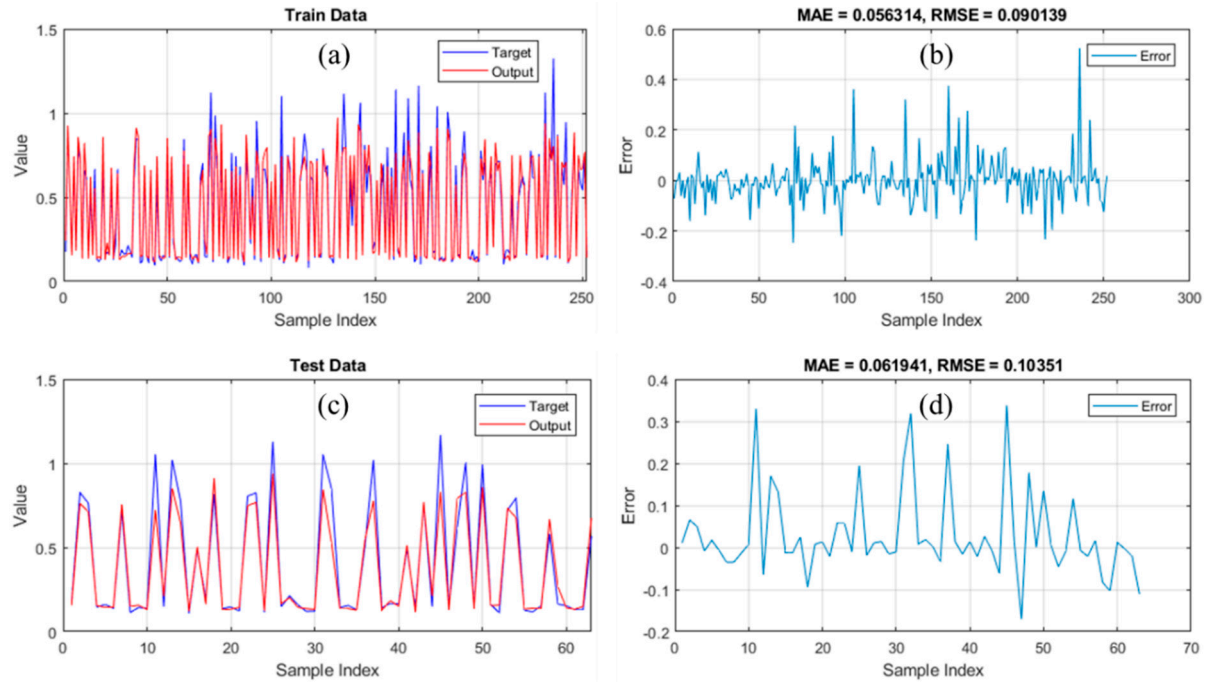

Figure 7. The ALO–ANN results for the (**a**,**b**) training and (**c**,**d**) testing data.

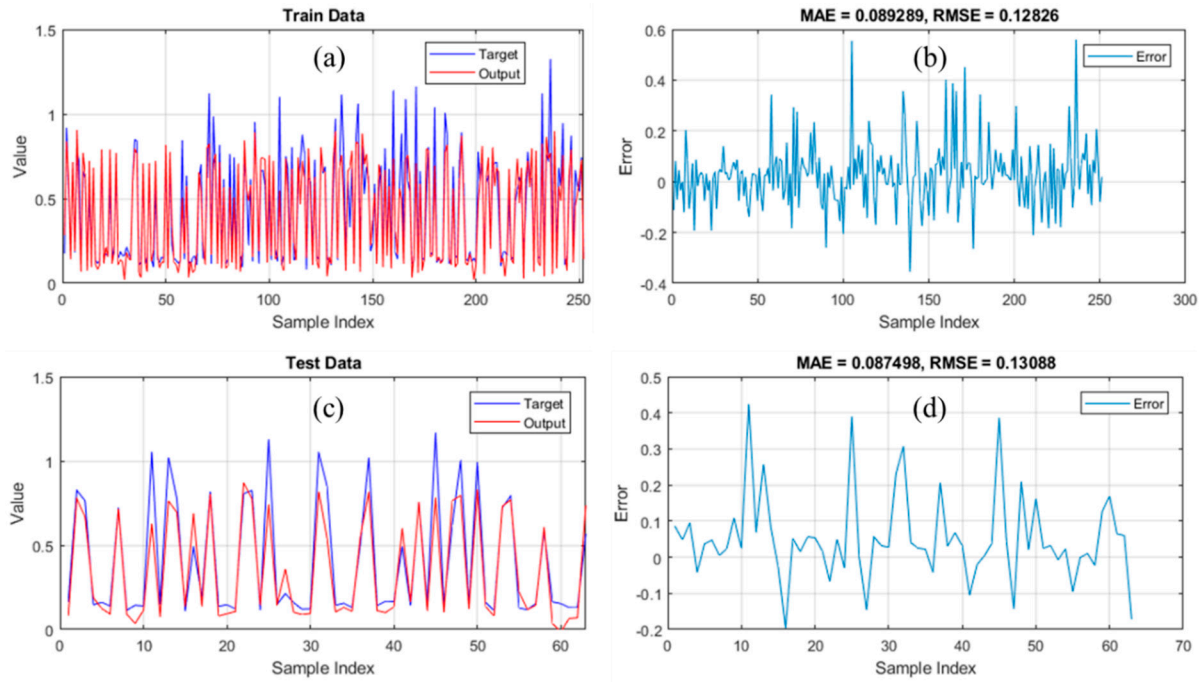

Figure 8. The SHO–ANN results for the (**a**,**b**) training and (**c**,**d**) testing data.

As well as the error criteria, the R^2 is used to measure the consistency of the results in terms of the correlation. Figure 9 shows the regression charts of the training and testing data of the implemented models. It can be seen that in both phases, the ALO and SHO enhanced the ANN, due to the higher consistency of their outputs with actual SSSs. The R^2 was raised from 0.8076 to 0.9155 and 0.8371 in the training phase, and from 0.8410 to 0.9348 and 0.8866 in the testing phase. Illustrated in the charts below, the actual training SSSs vary from 0.0843 to 1.3257, while the values predicted by the ANN, ALO–ANN, and SHO–ANN were in the range [0.1296–0.8890], [0.1128–0.9682], and [0.0222–0.9043], respectively. Similarly, the actually tested SSSs vary from 0.1114 to 1.1650, while the values predicted by the ANN, ALO–ANN, and SHO–ANN were in the range [0.0995–0.8426], [0.1170–0.9336], and [−0.0155–0.8714]. Although the negative values of shear strength do not make sense, one negative value (−0.0155) was obtained in the testing phase of the SHO–ANN, which is negligible. Considering that this negative value is attributed to one of the lowest values of WD, the reasons for its appearance could be sought in the mean correlation between the SSS and WD (correlation = 0.85). As well as this, the mechanism of neural computing might be another possible reason (which is out of the scope of the current paper).

Analyzing the results of the employed models reveals that utilizing both ALO and SHO is helpful for improving the capability of learning and predicting the SSS pattern. The comparison between the accuracy indices obtained for the ALO- and SHO-based ensembles shows that the ALO–ANN performed more promisingly, as it produced the outputs with lower error and a higher correlation with actual SSSs. In other words, the weights and biases suggested by the ALO constructed a more reliable ANN than those found by the SHO. This is also true regarding the generalization capability of the ANN reinforced by the ALO, because it produced more consistent results in the testing phase.

Although the running time taken by the ALO was nearly three times larger than the SHO, it provided a considerably more accurate approach. Also, despite the fact that previous studies have demonstrated the superiority of intelligent models (to traditional approaches) in terms of time-effectiveness, the significance of time as a source in engineering works drives us to constantly seek more efficient models. Figure 10 shows the comparison between the computation time (and the obtained objective function) of the proposed ALO–ANN and some well-known optimization techniques, namely the dragonfly algorithm (DA) [54], Harris hawks optimization (HHO) [55], artificial bee colony (ABC) [56], imperialist competitive algorithm (ICA) [57], elephant herding optimization

(EHO) [58], and PSO [59]. As can be observed, the ALO grasps the least objective function (i.e., the highest accuracy) in the lowest time.

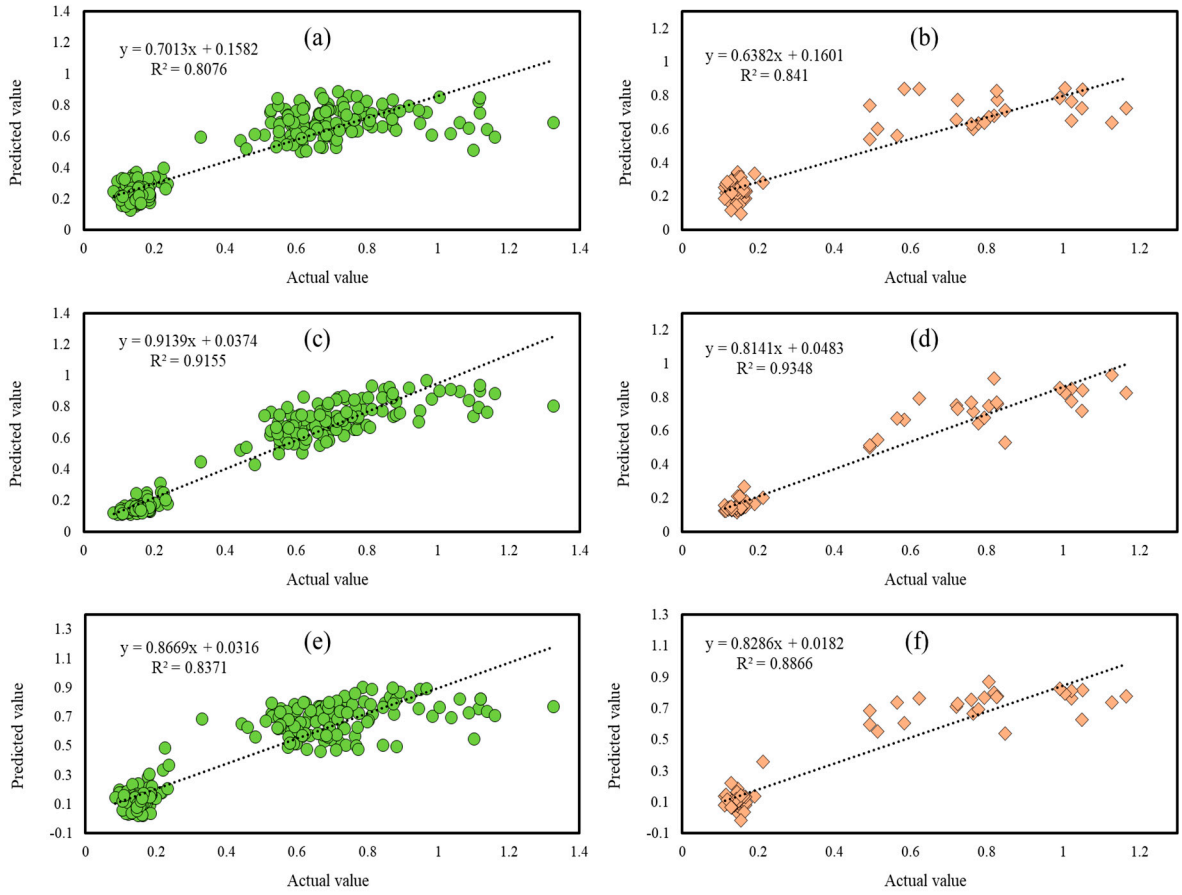

Figure 9. The correlation between the actual and predicted SSS in the training and testing phases of (**a**,**b**) ANN, (**c**,**d**) ALO–ANN, and (**e**,**f**) SHO–ANN.

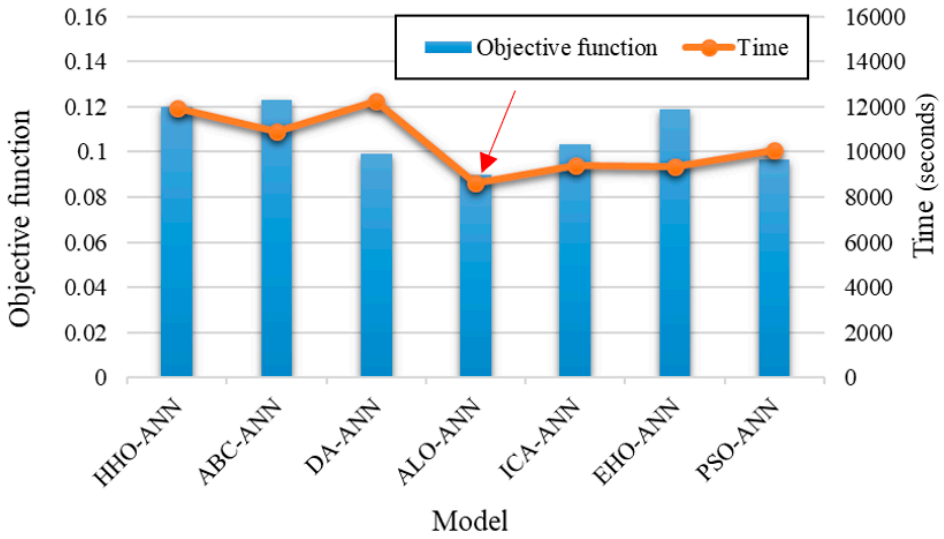

Figure 10. The comparison between the proposed ALO–ANN model and some optimization techniques in terms of computation time and objective function.

The applicability of the applied algorithms has been previously demonstrated for other optimization aims. In research by Kose [49] and Francis and Meganathan [60], for example, the ALO was used to improve the performance of the ANN and ANFIS, respectively. The SHO was similarly used by Li et al. [61] to train a feed-forward neural network for a heart-related classification problem. This work was done for tackling the drawbacks of the neural network, such as the fall into local optima. In research by Jia et al. [45], the SHO was employed to select features. However, the optimal solutions it found were enhanced by an embedded simulated annealing algorithm.

Lastly, due to the outcome of the ALO–ANN surpassing both the SHO–ANN and typical ANN, the mathematical relationship of this model is presented by Equation (10) as the SSS predictive formula. Remarkably, this formula is based on ten soil parameters that were considered for a specific study area, and it might be deemed as a limitation. This equation represents the weights and biases belonging to the unique output layer of the MLP optimized by the ALO. As can be observed, producing the response entails calculating some middle parameters, namely A, B, ... , F, which show the outputs released by the hidden neurons.

$$SSS_{ALO\text{-}ANN} = 0.9537 \times A - 0.1273 \times B + 0.2687 \times C - 0.3042 \times D - 0.9837 \times E + 0.7428 \tag{10}$$

$$\begin{bmatrix} A \\ B \\ C \\ D \\ E \end{bmatrix} = Tansig\left(\left(\begin{bmatrix} -0.5501 & 0.4989 & -0.7100 & 0.5843 & 0.5614 & 0.1942 & -0.6275 & -0.6038 & -0.1739 & -0.4073 \\ -0.4067 & -0.3411 & 0.0191 & 0.7350 & -0.5237 & 0.5284 & -0.6897 & 0.3148 & 0.7124 & -0.4960 \\ 0.6531 & -0.4407 & 0.4758 & 0.5773 & 0.3957 & 0.5426 & -0.1231 & -0.4806 & -0.9090 & -0.0235 \\ -0.4803 & -0.3584 & -0.3327 & -0.2229 & -0.3843 & -0.1481 & -1.0595 & 0.3627 & 0.6494 & 0.5824 \\ 0.5282 & 0.7723 & -0.5272 & 0.0430 & 0.6133 & 0.0413 & 0.4040 & 0.2355 & 0.0938 & -0.9714 \end{bmatrix} \begin{bmatrix} DOS \\ Sand \\ Loam \\ Clay \\ MC \\ WD \\ LL \\ PL \\ PI \\ LI \end{bmatrix}\right) + \begin{bmatrix} 1.6445 \\ 0.8222 \\ 0.0000 \\ -0.8222 \\ 1.6445 \end{bmatrix}\right) \tag{11}$$

$$Tansig\ (x) = \frac{2}{1 + e^{-2x}} - 1 \tag{12}$$

5. Conclusions

The importance of assessing crucial parameters of the soil, such as shear strength, is obvious for various engineering projects. The applicability of two novel optimization methods, namely ALO and SHO, was investigated for their shear strength prediction when incorporated into an artificial neural network. These techniques were used to find the most appropriate computational parameters (i.e., the weights and biases) of the ANN. After determining the best complexity of the models, it was shown that the elite structure of the ALO–ANN needs double the population of the SHO–ANN. Assessment of the results using the RMSE, MAE, and R^2 demonstrated that the ANN constructed by the hybrid algorithms enjoys more accuracy than its unreinforced version. Furthermore, the ALO showed higher robustness compared to the SHO, as well as several hybrid models trialed in earlier studies. Meanwhile, extracting the SSS predictive formula of the best model (i.e., the ALO–ANN) was an additional achievement of this work. Overall, the adequacy of artificial intelligence techniques along with swarm-based optimization techniques for modeling the soil shear strength was derived in this

study, and the authors believe that the suggested ALO–ANN is accurate enough to be an alternative to traditional evaluation models.

Author Contributions: H.M. and D.T.B. performed experiments and field data collection; H.M., B.K., and D.A. wrote the manuscript, discussion and analyzed the data.

Funding: This research received no external funding.

Acknowledgments: This work was financially supported by Ton Duc Thang University.

Conflicts of Interest: The authors declare no conflict of interest.

References

1. Moavenian, M.; Nazem, M.; Carter, J.; Randolph, M. Numerical analysis of penetrometers free-falling into soil with shear strength increasing linearly with depth. *Comput. Geotech.* **2016**, *72*, 57–66. [CrossRef]
2. Moayedi, H.; Hayati, S. Modelling and optimization of ultimate bearing capacity of strip footing near a slope by soft computing methods. *Appl. Soft Comput.* **2018**, *66*, 208–219. [CrossRef]
3. Alnaqi, A.A.; Moayedi, H.; Shahsavar, A.; Nguyen, T.K. Prediction of energetic performance of a building integrated photovoltaic/thermal system thorough artificial neural network and hybrid particle swarm optimization models. *Energy Convers. Manag.* **2018**, *183*, 137–148. [CrossRef]
4. Vanapalli, S.; Fredlund, D. Comparison of different procedures to predict unsaturated soil shear strength. In *Advances in Unsaturated Geotechnics*; ASCE: Reston, VA, USA, 2000; pp. 195–209.
5. Aksoy, H.S.; Gor, M. High-speed railway embankments stabilization by using a plant based biopolymer. *Fresenius Environ. Bull.* **2017**, *25*, 7626–7633.
6. Das, B.M.; Sobhan, K. *Principles of Geotechnical Engineering*; Cengage Learning: Boston, MA, USA, 2013.
7. Nhu, V.-H.; Hoang, N.-D.; Duong, V.-B.; Vu, H.-D.; Bui, D.T. A hybrid computational intelligence approach for predicting soil shear strength for urban housing construction: A case study at Vinhomes Imperia project, Hai Phong city (Vietnam). *Eng. Comput.* **2019**, 1–14. [CrossRef]
8. Nam, S.; Gutierrez, M.; Diplas, P.; Petrie, J. Determination of the shear strength of unsaturated soils using the multistage direct shear test. *Eng. Geol.* **2011**, *122*, 272–280. [CrossRef]
9. Rassam, D.W.; Williams, D.J. A relationship describing the shear strength of unsaturated soils. *Can. Geotech. J.* **1999**, *36*, 363–368. [CrossRef]
10. Gan, J.; Fredlund, D.; Rahardjo, H. Determination of the shear strength parameters of an unsaturated soil using the direct shear test. *Can. Geotech. J.* **1988**, *25*, 500–510. [CrossRef]
11. Bui, D.T.; Moayedi, H.; Gör, M.; Jaafari, A.; Foong, L.K. Predicting slope stability failure through machine learning paradigms. *ISPRS Int. J. Geo-Inf.* **2019**, *8*, 395. [CrossRef]
12. Moayedi, H.; Bui, D.T.; Gör, M.; Pradhan, B.; Jaafari, A. The feasibility of three prediction techniques of the artificial neural network, adaptive neuro-fuzzy inference system, and hybrid particle swarm optimization for assessing the safety factor of cohesive slopes. *ISPRS Int. J. Geo-Inf.* **2019**, *8*, 391. [CrossRef]
13. Müller, R.; Larsson, S.; Spross, J. Extended multivariate approach for uncertainty reduction in the assessment of undrained shear strength in clays. *Can. Geotech. J.* **2013**, *51*, 231–245. [CrossRef]
14. Vanapalli, S.; Fredlund, D. Empirical procedures to predict the shear strength of unsaturated soils. In Proceedings of the Eleventh Asian Regional Conference on Soil Mechanics and Geotechnical Engineering, Seoul, Korea, 16–20 August 1999; pp. 93–96.
15. Zhai, Q.; Rahardjo, H.; Satyanaga, A.; Dai, G. Estimation of unsaturated shear strength from soil–water characteristic curve. *Acta Geotech.* **2019**, 1–14. [CrossRef]
16. Al Aqtash, U.; Bandini, P. Prediction of unsaturated shear strength of an adobe soil from the soil–water characteristic curve. *Constr. Build. Mater.* **2015**, *98*, 892–899. [CrossRef]
17. Garven, E.; Vanapalli, S. Evaluation of empirical procedures for predicting the shear strength of unsaturated soils. In *Unsaturated Soils 2006*; ASCE: Reston, VA, USA, 2006; pp. 2570–2592.
18. Kiran, S.; Lal, B.; Tripathy, S. Shear strength prediction of soil based on probabilistic neural network. *Indian J. Sci. Technol.* **2016**, *9*. [CrossRef]
19. Jokar, M.H.; Mirasi, S. Using adaptive neuro-fuzzy inference system for modeling unsaturated soils shear strength. *Soft Comput.* **2018**, *22*, 4493–4510. [CrossRef]

20. Kanungo, D.; Sharma, S.; Pain, A. Artificial Neural Network (ANN) and Regression Tree (CART) applications for the indirect estimation of unsaturated soil shear strength parameters. *Front. Earth Sci.* **2014**, *8*, 439–456. [CrossRef]
21. Besalatpour, A.; Hajabbasi, M.; Ayoubi, S.; Afyuni, M.; Jalalian, A.; Schulin, R. Soil shear strength prediction using intelligent systems: Artificial neural networks and an adaptive neuro-fuzzy inference system. *Soil Sci. Plant Nutr.* **2012**, *58*, 149–160. [CrossRef]
22. Taherdangkoo, M.; Taherdangkoo, R. Modified BNMR algorithm applied to Loney's solenoid benchmark problem. *Int. J. Appl. Electromagn. Mech.* **2014**, *46*, 683–692. [CrossRef]
23. Qiu, P.; Hu, R.; Hu, L.; Liu, Q.; Xing, Y.; Yang, H.; Qi, J.; Ptak, T. A Numerical Study on Travel Time Based Hydraulic Tomography Using the SIRT Algorithm with Cimmino Iteration. *Water* **2019**, *11*, 909. [CrossRef]
24. Moayedi, H.; Mehrabi, M.; Mosallanezhad, M.; Rashid, A.S.A.; Pradhan, B. Modification of landslide susceptibility mapping using optimized PSO-ANN technique. *Eng. Comput.* **2018**, *35*, 967–984. [CrossRef]
25. Gao, W.; Dimitrov, D.; Abdo, H. Tight independent set neighborhood union condition for fractional critical deleted graphs and ID deleted graphs. *Discret. Contin. Dyn. Syst. Ser. S* **2018**, *12*, 711–721. [CrossRef]
26. Nguyen, H.; Mehrabi, M.; Kalantar, B.; Moayedi, H.; Abdullahi, M.A.M. Potential of hybrid evolutionary approaches for assessment of geo-hazard landslide susceptibility mapping. *Geomat. Nat. Hazards Risk* **2019**, *10*, 1667–1693. [CrossRef]
27. Gao, W.; Guirao, J.L.G.; Basavanagoud, B.; Wu, J. Partial multi-dividing ontology learning algorithm. *Inf. Sci.* **2018**, *467*, 35–58. [CrossRef]
28. Moayedi, H.; Mehrabi, M.; Kalantar, B.; Abdullahi Mu'azu, M.A.; Rashid, A.S.; Foong, L.K.; Nguyen, H. Novel hybrids of adaptive neuro-fuzzy inference system (ANFIS) with several metaheuristic algorithms for spatial susceptibility assessment of seismic-induced landslide. *Geomat. Nat. Hazards Risk* **2019**, *10*, 1879–1911. [CrossRef]
29. Tien Bui, D.; Khosravi, K.; Li, S.; Shahabi, H.; Panahi, M.; Singh, V.; Chapi, K.; Shirzadi, A.; Panahi, S.; Chen, W. New hybrids of anfis with several optimization algorithms for flood susceptibility modeling. *Water* **2018**, *10*, 1210. [CrossRef]
30. Bui, D.T.; Hoang, N.-D.; Nhu, V.-H. A swarm intelligence-based machine learning approach for predicting soil shear strength for road construction: A case study at Trung Luong National Expressway Project (Vietnam). *Eng. Comput.* **2019**, *35*, 955–965.
31. Pham, B.T.; Hoang, T.-A.; Nguyen, D.-M.; Bui, D.T. Prediction of shear strength of soft soil using machine learning methods. *Catena* **2018**, *166*, 181–191. [CrossRef]
32. McCulloch, W.S.; Pitts, W. A logical calculus of the ideas immanent in nervous activity. *Bull. Math. Biophys.* **1943**, *5*, 115–133. [CrossRef]
33. ASCE Task Committee. Artificial neural networks in hydrology. II: Hydrologic applications. *J. Hydrol. Eng.* **2000**, *5*, 124–137. [CrossRef]
34. Moayedi, H.; Hayati, S. Applicability of a CPT-Based Neural Network Solution in Predicting Load-Settlement Responses of Bored Pile. *Int. J. Geomech.* **2018**, *18*, 06018009. [CrossRef]
35. Seyedashraf, O.; Mehrabi, M.; Akhtari, A.A. Novel approach for dam break flow modeling using computational intelligence. *J. Hydrol.* **2018**, *559*, 1028–1038. [CrossRef]
36. Gao, W.; Guirao, J.L.G.; Abdel-Aty, M.; Xi, W. An independent set degree condition for fractional critical deleted graphs. *Discret. Contin. Dyn. Syst. Ser. S* **2019**, *12*, 877–886. [CrossRef]
37. Gao, W.; Wang, W.; Dimitrov, D.; Wang, Y. Nano properties analysis via fourth multiplicative ABC indicator calculating. *Arab. J. Chem.* **2018**, *11*, 793–801. [CrossRef]
38. Gao, W.; Wu, H.; Siddiqui, M.K.; Baig, A.Q. Study of biological networks using graph theory. *Saudi J. Biol. Sci.* **2018**, *25*, 1212–1219. [CrossRef] [PubMed]
39. Hecht-Nielsen, R. Theory of the backpropagation neural network. In *Neural Networks for Perception*; Elsevier: Washington, DC, USA, 1992; pp. 65–93.
40. Moré, J.J. The Levenberg-Marquardt algorithm: Implementation and theory. In *Numerical Analysis*; Springer: Berlin/Heidelberg, Germany, 1978; pp. 105–116.
41. Rizeei, H.M.; Pradhan, B.; Saharkhiz, M.A. An integrated fluvial and flash pluvial model using 2D high-resolution sub-grid and particle swarm optimization-based random forest approaches in GIS. *Complex Intell. Syst.* **2018**, *5*, 283–302. [CrossRef]

42. Mojaddadi, H.; Pradhan, B.; Nampak, H.; Ahmad, N.; Ghazali, A.H.B. Ensemble machine-learning-based geospatial approach for flood risk assessment using multi-sensor remote-sensing data and GIS. *Geomat. Nat. Hazards Risk* **2017**, *8*, 1080–1102. [CrossRef]
43. Dhiman, G.; Kumar, V. Multi-objective spotted hyena optimizer: A Multi-objective optimization algorithm for engineering problems. *Knowl. Based Syst.* **2018**, *150*, 175–197. [CrossRef]
44. Luo, Q.; Li, J.; Zhou, Y. Spotted hyena optimizer with lateral inhibition for image matching. *Multimed. Tools Appl.* **2019**, *78*, 1–20. [CrossRef]
45. Jia, H.; Li, J.; Song, W.; Peng, X.; Lang, C.; Li, Y. Spotted Hyena Optimization Algorithm with Simulated Annealing for Feature Selection. *IEEE Access* **2019**, 71943–71962. [CrossRef]
46. Kaur, A.; Kaur, S.; Dhiman, G. A quantum method for dynamic nonlinear programming technique using Schrödinger equation and Monte Carlo approach. *Mod. Phys. Lett. B* **2018**, *32*, 1850374. [CrossRef]
47. Mirjalili, S. The ant lion optimizer. *Adv. Eng. Softw.* **2015**, *83*, 80–98. [CrossRef]
48. Špoljarić, T.; Pavić, I. Performance analysis of an ant lion optimizer in tuning generators' excitation controls in multi machine power system. In Proceedings of the 2018 41st International Convention on Information and Communication Technology, Electronics and Microelectronics (MIPRO), Opatija, Croatia, 21–25 May 2018; pp. 1040–1045.
49. Kose, U. An ant-lion optimizer-trained artificial neural network system for chaotic electroencephalogram (EEG) prediction. *Appl. Sci.* **2018**, *8*, 1613. [CrossRef]
50. Mirjalili, S.; Jangir, P.; Saremi, S. Multi-objective ant lion optimizer: A multi-objective optimization algorithm for solving engineering problems. *Appl. Intell.* **2017**, *46*, 79–95. [CrossRef]
51. ASTM. *Standard Test Method for Laboratory Miniature Vane Shear Test for Saturated Fine-Grained Clayey Soil*; ASTM: West Conshohocken, PA, USA, 2005.
52. Schmertmann, J.H. *Guidelines for Cone Penetration Test: Performance and Design*; Federal Highway Administration: Washington, DC, USA, 1978.
53. Clayton, C.R. *The Standard Penetration Test (SPT): Methods and Use*; Construction Industry Research and Information Association (CIRIA): London, UK, 1995.
54. Mirjalili, S. Dragonfly algorithm: A new meta-heuristic optimization technique for solving single-objective, discrete, and multi-objective problems. *Neural Comput. Appl.* **2016**, *27*, 1053–1073. [CrossRef]
55. Heidari, A.A.; Mirjalili, S.; Faris, H.; Aljarah, I.; Mafarja, M.; Chen, H. Harris hawks optimization: Algorithm and applications. *Future Gener. Comput. Syst.* **2019**, *97*, 849–872. [CrossRef]
56. Karaboga, D. *An Idea Based on Honey Bee Swarm for Numerical Optimization*; Technical report-tr06; Computer Engineering Faculty, Erciyes University: Kayseri, Turkey, 2005.
57. Atashpaz-Gargari, E.; Lucas, C. Imperialist competitive algorithm: An algorithm for optimization inspired by imperialistic competition. In Proceedings of the 2007 IEEE Congress on Evolutionary Computation, Singapore, 25–28 September 2007; pp. 4661–4667.
58. Wang, G.-G.; Deb, S.; Coelho, L.D.S. Elephant herding optimization. In Proceedings of the 2015 3rd International Symposium on Computational and Business Intelligence (ISCBI), Bali, Indonesia, 7–9 December 2015; pp. 1–5.
59. Eberhart, R.; Kennedy, J. Particle swarm optimization. In Proceedings of the IEEE International Conference on Neural Networks, Perth, Western Australia, 27 November–1 December 1995; pp. 1942–1948.
60. Francis, R.; Meganathan, D. An improved ANFIS with aid of ALO technique for THD minimization of multilevel inverters. *J. CircuitsSyst. Comput.* **2018**, *27*, 1850193. [CrossRef]
61. Li, J.; Luo, Q.; Liao, L.; Zhou, Y. Using Spotted Hyena Optimizer for Training Feedforward Neural Networks. In *International Conference on Intelligent Computing*; Springer: Wuhan, China, 2018; pp. 828–833.